IJIREEICE

ISSN (Online) 2321-2004
ISSN (Print) 2321-5526

International Journal of Innovative Research in
Electrical, Electronics, Instrumentation and Control Engineering

Vol. 9, Issue 6, June 2021

DOI 10.17148/IJIREEICE.2021.9636

Two Stage Three Phase Grid Connected VSI with SEPIC Converter and Incremental Conductance based MPPT Algorithm for PV Systems

SUJAY N R[1], Dr. DINESH M N[2]

PG Student, Department of EEE, R V College of Engineering, Bengaluru, India[1]

Associate Professor, Department of EEE, R V College of Engineering, Bengaluru, India[2]

Abstract: In recent days the Photovoltaic (PV) systems have been acknowledged as a key source of renewable energy. The amount of solar irradiation and cell operating temperature affect the electricity generated by the PV system due to the unpredictable fluctuations in environmental patterns. As a result, the grid-integrated PV system was proposed in this paper in order to extract maximum power from the PV array in order to meet load requirements, also supplying surplus electricity to the AC grid. Maximum power point tracking (MPPT) of the non-uniformly irradiated PV array, conversion efficiency maximization, and grid synchronization are the major design goals. This paper explores new MPPT control algorithms using the modified incremental conductance approach, which improves the performance and reduces the error, allowing for more efficient power extraction from solar arrays. In addition, network stability, power quality, and grid synchronization functionalities for PV grid-connected systems are implemented. The control of the voltage source converter was designed in such a way that PV power generated is synchronous to the grid. The typical waveforms of grid voltage, grid current and harmonics of grid current are carried out on a 100kW photovoltaic inverter, which will provide some guidelines in order to analyse, design and implement.
In Matlab/Simulink, modelling of various controllers was carried out to obtain improved efficient power extraction, grid synchronization, and minimal performance loss owing to dynamic tracking errors, especially under fast-changing irradiation. Variation in atmospheric condition was simulated, by gradually varying the different parameters like irradiation and temperature of PV module in order to verify the performance of the proposed Incremental Conductance (INC) algorithm, and different controllers of the converters. The performance of the proposed system is obtained satisfactorily and matches closely to the theoretical values. The over efficiency of the proposed system obtained is 98%-99% and the THD levels is less than 1.5% which meets the requisite standards to integrate PV systems into grid.

Keywords: Photovoltaic (PV)**,** Incremental Conductance (INC), Maximum Power Point Tracking(MPPT), Voltage Source Inverter(VSI), Proportional Integral Derivative (PID), Phase Locked Loop (PLL), Synchronous Pulse Width Modulation (PWM), Voltage source Inverter (VSI), Total Harmonic Distortion (THD).

I. INTRODUCTION

In recent days the use of renewable energy is widely increasing day by day. Among them, Solar Energy is considered as one of the important Energy sources since they are environmental friendly and produces electric power without causing pollution. Therefore, Solar Photo Voltaic (PV) panels is preferred that are readily available. According to the functions and configuration, photovoltaic power systems are classified in two types first is Standalone system and second is Grid connected systems. The standalone system required battery back-ups to achieve the MPPT and also it is independent of the utility grid. Therefore, the grid connected systems have been increasing that supply solar power to the utility grid. Because of their application in distributed generation, PV that is connected to grid has been used

Generally, the system that are connected to the grid are of two stages, the first stage is dc-to-dc converters that boosts the PV voltages and extract the Maximum Power by utilizing MPPT and the stage two is to invert this DC power to AC power. The Maximum Power Point Tracking (MPPT) algorithm is used to track the maximum power from solar array. In proposed system it reduces complexity, less weight, low cost, high efficiency and Sinusoidal Current is injected into the Grid. Since the PV modules cannot be connected directly to the grid, several studies have been proposed on

This work is licensed under a Creative Commons Attribution 4.0 International License

IJIREEICE
ISSN (Online) 2321-2004
ISSN (Print) 2321-5526
International Journal of Innovative Research in
Electrical, Electronics, Instrumentation and Control Engineering
Vol. 9, Issue 6, June 2021
DOI 10.17148/IJIREEICE.2021.9636

maximum power point tracking (MPPT) algorithms, DC-DC converter and inverter topologies and current control schemes have been proposed for the grid connected PV applications.

II. BLOCK DIAGRAM OF THE PROPOSED SYSTEM

The Block diagram of the system to connect the solar system with the utility grid is depicted in Fig.1. In the first stage, the solar generator's output is connected to a SEPIC converter, which raises or reduces the PV's voltage to a level acceptable for the DC to AC inverter by using the signals generated from Maximum power point tracking algorithm that is given to the switch of the SEPIC converter through PWM generator and to maintain the PV array to operate at optimal MPP.

The second stage is the inverter that converts DC power to three-phase power to serve the grid. The inverter is set to control currents. The inverter's output is filtered with an LCL filter to reduce the harmonics produced by the inverter, and is controlled by a high frequency PWM. The inverter's control goal is to synchronize the frequency and phases between the grid and the PV, as well as to maintain a steady DC bus voltage. As a result, inverter control enables for a unitary power factor side grid.

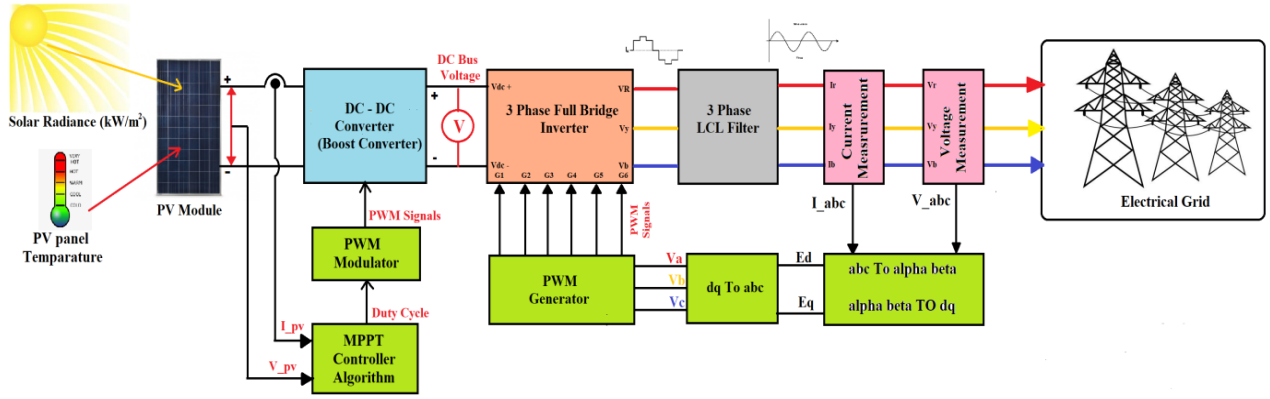

Fig.1 Block diagram of the proposed system

III. DESIGN OF PROPOSED SYSTEM

A. Photo Voltaic Module

A photovoltaic module is a collection of solar cells that are electrically connected and housed on a support structure or frame. Modules are made to deliver electricity at a specific voltage. An array is formed by connecting several PV modules. In general, the greater a module or array's surface area is, the more electricity it produces. For generating a desired voltage and current the modules are coupled in both series and parallel electrical configurations.

The Table 1 gives the detail specification of the built-in Simulink 1Soltech 1 STH 215P module used in the project.

TABLE I, Specification of the PV module 1Soltech 1 STH 215P

Sl no	Parameter	Unit	Values
1	Maximum Power	Watt	213.15
2	Cells per module	No	60
3	Open circuit voltage	Voc (V)	36.3
4	Short circuit current	Isc (A)	7.84
5	Voltage at Maximum Power point	Vmpp (V)	29
6	Current at Maximum Power point	Impp (A)	7.35
7	Temperature coefficient of Voc	%/°C	-0.36099
8	Temperature coefficient of Isc	%/°C	0.102

This work is licensed under a Creative Commons Attribution 4.0 International License

IJIREEICE
International Journal of Innovative Research in
Electrical, Electronics, Instrumentation and Control Engineering
ISSN (Online) 2321-2004
ISSN (Print) 2321-5526
Vol. 9, Issue 6, June 2021
DOI 10.17148/IJIREEICE.2021.9636

Even though PV array modeling may be done with Simulink simple components, MATLAB includes a built-in PV array block. For the simulation, the built-in Simulink 1Soltech 1 STH 215P module is used, with each module capable of producing 213.15Watts of power. As a result, a PV block for a 100 KW output power from the PV array under standard test conditions (STC) requires 470 solar modules with 47 parallel string connections and 10 series string connections, resulting in an average power of 47 x 10 x 213.15Watts (maximum power obtained from each PV panel) = 100.18 kW at 25 °C or STC.

By considering the specification of the PV module in the Table 1, the values indicated is for single PV Module. Since the prototype is designed for 100kW rating the, total specification is give below,

1. Open circuit Voltage of the Complete string = 36.3 x 10 = 363 V
2. Short circuit current of the Complete string = 7.84 x 47 = 368.48 A
3. Voltage at Maximum Power point of the string = 29 x 10 = 290 V
4. Current at Maximum Power point of the string = 7.35 x 47 = 345.45 A

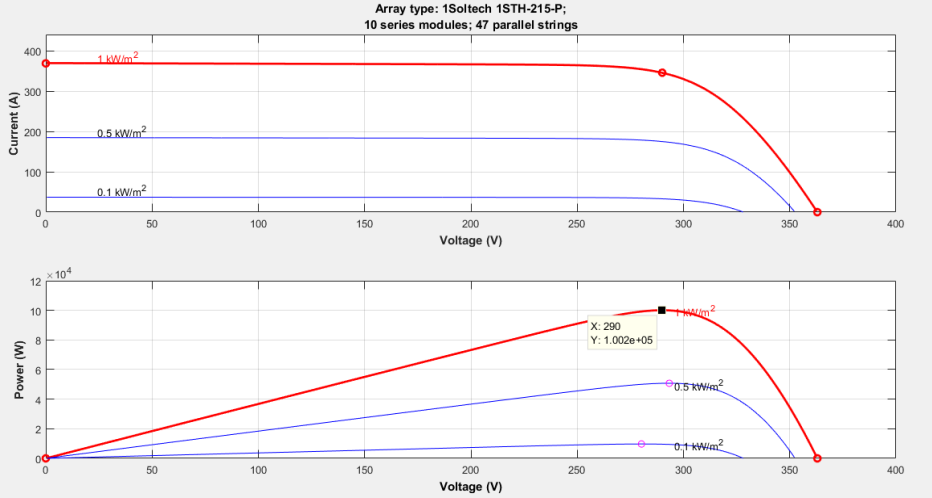

Fig. 2 Current (I) & Power (P) vs. Voltage (V) graph of the PV array (1Soltec 1STH-215-P) for the different values of Irradiation at STC.

The Fig.2 depicts a study of PV output voltage vs. current characteristics for various irradiances. The graphs illustrate that the PV module's output current is proportional to the amount of irradiation. Also the irradiance has an effect on the PV module's voltage vs. power. The overall performance is poor as the amount of irradiance decreases.

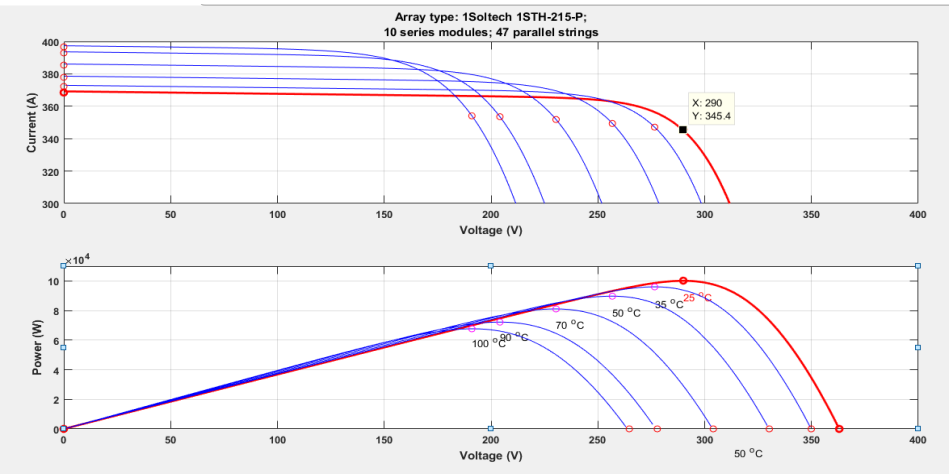

This work is licensed under a Creative Commons Attribution 4.0 International License

IJIREEICE
ISSN (Online) 2321-2004
ISSN (Print) 2321-5526
International Journal of Innovative Research in
Electrical, Electronics, Instrumentation and Control Engineering
Vol. 9, Issue 6, June 2021
DOI 10.17148/IJIREEICE.2021.9636

Fig.3 Current (I) & Power (P) vs. Voltage (V) graph of the PV array (1Soltec 1STH-215-P) for different internal temperature of PV module at constant irradiation

Fig.3 depicts the results of an investigation based on the effects of temperature on the PV array. The output voltage and current of a PV array is affected by temperature. The PV panels performance is degraded when the temperatures rises.

B. Design of SEPIC Converter

The SEPIC converter produces an output voltage like buck boost converter, furthermore its polarity could be reversed, the design SEPIC converter includes the next features, the design parameter considered for the design of the SEPIC converter is given in Table 2,

The output current is calculated as,

$$I_o = \frac{P}{V_o} = \frac{100kW}{600\ V} = 166.6\ Amps$$

TABLE II, Design Parameter for SEPIC converter

Sl no	Parameter	Values
1	Input Voltage (Vs min)	290 V
2	Input Voltage (Vs max)	363 V
3	Input current (Is)	345.45 A
4	Output Voltage (Vo)	600V
5	Power (P)	100kW

1) Duty cycle calculation

Duty cycle is calculated based on converter operation continuous mode, where $V_D = 0.5$

$$D_{min} = \frac{V_{out} + V_D}{V_{s(max)} + V_{out} + V_{in}} \quad (1)$$

$$D_{min} = \frac{600 + 0.5}{363 + 600 + 0.5}$$

$$D_{min} = 0.623$$

$$D_{max} = \frac{V_{out} + V_D}{V_{s(min)} + V_{out} + V_{in}} \quad (2)$$

$$D_{max} = \frac{600 + 0.5}{290 + 600 + 0.5}$$

$$D_{max} = 0.674$$

2) Inductance Calculation

The peak to peak ripple current to be approximately 40% of the maximum input current at the minimum input voltage.

$$\Delta I_L = I_{out}\left(\frac{V_{out}}{V_{s(min)}}\right)40\% \quad (3)$$

$$\Delta I_L = 166.6\left(\frac{600}{290}\right)\text{x } 0.4$$

This work is licensed under a Creative Commons Attribution 4.0 International License

IJIREEICE
ISSN (Online) 2321-2004
ISSN (Print) 2321-5526
International Journal of Innovative Research in
Electrical, Electronics, Instrumentation and Control Engineering
Vol. 9, Issue 6, June 2021
DOI 10.17148/IJIREEICE.2021.9636

$$\Delta I_L = 137.8\ A$$

The inductor value is calculated as,

$$L_1 = L_2 = L = \left(\frac{V_{S(min)}}{\Delta I_L x\, f}\right) D_{max} \tag{4}$$

$$L_1 = L_2 = L = \left(\frac{290}{137.8 \times 5000}\right) 0.674$$

$$L_1 = L_2 = L = 28.3\ \mu H$$

The peak current in the inductor, to ensure the inductor does not saturate, is given by,

$$I_{L1(peak)} = I_{out}\left(\frac{V_o + V_D}{V_{s(min)}}\right)\left(1 + \frac{40\%}{2}\right) \tag{5}$$

$$I_{L1(peak)} = 166.6\left(\frac{600 + 0.5}{290}\right) x\ 1.2$$

$$I_{L1(peak)} = 413.83\ A$$

$$I_{L2\ (peak)} = I_{out}\left(1 + \frac{40\%}{2}\right) \tag{6}$$

$$I_{L2\ (peak)} = 166.6 \times 1.2$$

$$I_{L2\ (peak)} = 199.92\ A$$

3) Capacitance Calculation

SEPIC coupling capacitor selection is given by,

$$I_{cs(min)} = I_o\left(\sqrt{\frac{V_{out} + V_D}{V_{s(min)}}}\right) \tag{7}$$

$$I_{cs(min)} = 239.73\ A$$

and the ripple voltage is

$$\Delta V_{Cs} = \frac{I_{out} x\, D_{max}}{C_s x\, f} \tag{8}$$

$$\Delta V_{Cs} = \frac{166.6 \times 0.674}{2000\mu \times 5000}$$

$$\Delta V_{Cs} = 10.37\ V$$

Assuming the peak-to-peak ripple is 0.2% of 600V output voltage and the value Cs is proposed as 2000 µf then the capacitance is given by,

$$C_{out} \geq \frac{I_{out} x\, D_{max}}{C_s x\, f} \tag{9}$$

$$C_{out} \geq \frac{166.5 \times 0.674}{2000\mu \times 5000}$$

$$C_{out} \geq 4000\mu F$$

This work is licensed under a Creative Commons Attribution 4.0 International License

IJIREEICE
ISSN (Online) 2321-2004
ISSN (Print) 2321-5526
International Journal of Innovative Research in
Electrical, Electronics, Instrumentation and Control Engineering
Vol. 9, Issue 6, June 2021
DOI 10.17148/IJIREEICE.2021.9636

C. Design of LCL Filter

The three phase LCL filter is depicted in Fig. 4. and connected after the VSI, later integrated to grid, the filter consist of 2sets of inductors per phase and a set of capacitors per phase, the design is as follows,

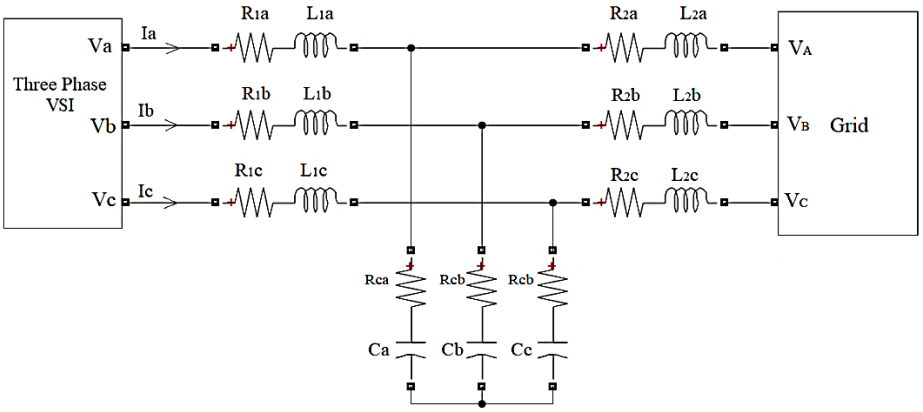

Fig.4 Three phase LCL filter

The Table 3 shows the values of different parameter that is taken into consideration in designing different components of the filter.

TABLE III, Value of parameter consider for filter design

Sl no	Parameter	Values
1	Total power (P_{rated})	100 kW
2	Grid voltage (V_{grid})	230 V
3	Grid current (I_{grid})	144.92 A
4	Frequency (f)	50 Hz

1) Design of Inductance

The value of Inductance is calculated based on Voltage drop across it. According to IEEE standards the voltage drop across the filter inductor is limited to 20% of the total voltage of the grid

$$\text{i.e, } V_L = 20\% \text{ of } V_{grid} \tag{10}$$

$$\text{So, } L = 0.2 \times \frac{V_{grid}}{2\pi \times f \times I}$$

$$L = 0.2 \times \frac{230}{2\pi \times 50 \times 144.92}$$

$$L = 1\text{mH}$$

$$L_1 = L_2 = 1\text{mH} / 2$$

$$L_1 = L_2 = 500\ \mu\text{H}$$

2) Design of Capacitor

Value of capacitance is designed by the value of Reactive power requirement of the Capacitor. Reactive Power observed by Capacitor is limited to 5% of the Rated Power.

$$\text{Reactive Power } Q = \frac{V^2}{\frac{1}{2\pi fc}} = 5\% \text{ of } S_{rated} \tag{11}$$

$$V^2 \times 2\pi fc = 5\% \text{ of } S_{rated}$$

This work is licensed under a Creative Commons Attribution 4.0 International License

IJIREEICE
ISSN (Online) 2321-2004
ISSN (Print) 2321-5526
International Journal of Innovative Research in
Electrical, Electronics, Instrumentation and Control Engineering
Vol. 9, Issue 6, June 2021
DOI 10.17148/IJIREEICE.2021.9636

$$C = \frac{0.05 \text{ x Srated}}{V^2 x\, 2\pi f} = \frac{0.05 \text{ x } (100k/3)}{230^2 x\, 2\pi \text{ x } 50}$$

$$C_1 = C_2 = C_3 = 100.28\ \mu f$$

IV. IMPLEMENTATION OF PROPOSED SYSTEM

A. Simulation of PV array and DC to DC converter with control block

The first stage of the proposed converter consists of the PV array and dc to dc converter that is designed as per parameters given in the Table 4. The PV module is arranged in such a way in order to get the output power of 100kW and the power is controlled by the environmental factors like Irradiation from the Sun and Internal temperature of the PV modules.

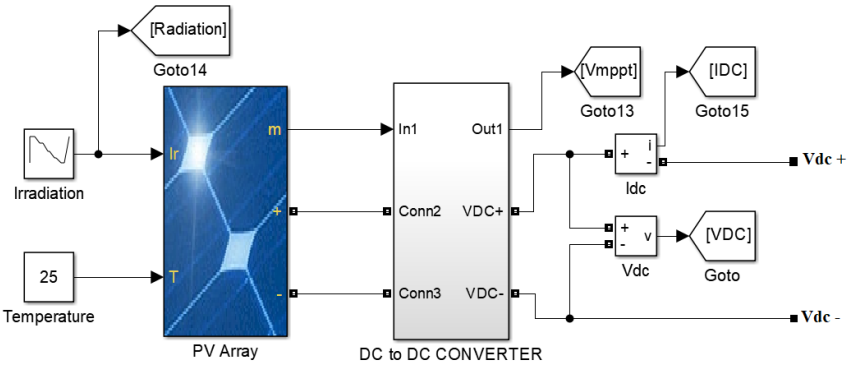

Fig.5 Implementation of first stage of the proposed converter

These two factors are given as the input to the PV module, which will be varied for different output power and study of the implementation of the MPPT logic. The Fig.5 depicts the implantation of the first stage of the proposed converter circuit in Matlab/Simulink.

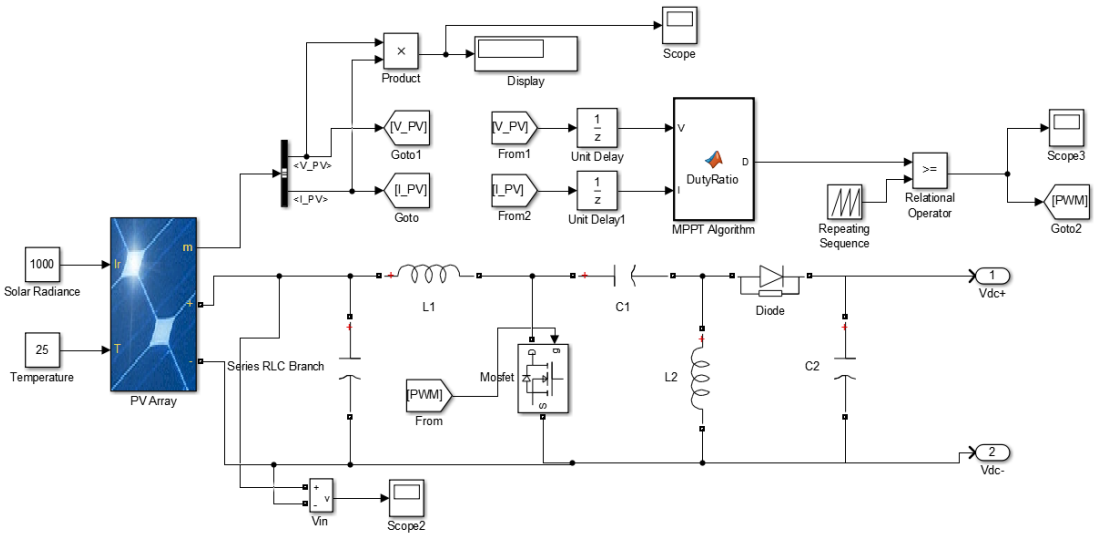

Fig.6 Implementation of MPPT logic and SEPIC converter

The DC to DC converter and the proposed MPPT algorithm is used for tracking the Maximum power point of the PV array by matching the output resistance with the internal resistance of the PV module, which is carried out by the process of adjusting the duty cycle of the switch. The SEPIC converter and the MPPT algorithm is built in the dc to dc converter block, which also helps to keep the dc link voltage stable and extract the Maximum power from the PV array

This work is licensed under a Creative Commons Attribution 4.0 International License

IJIREEICE
ISSN (Online) 2321-2004
ISSN (Print) 2321-5526
International Journal of Innovative Research in
Electrical, Electronics, Instrumentation and Control Engineering
Vol. 9, Issue 6, June 2021
DOI 10.17148/IJIREEICE.2021.9636

with respect to the varying environmental conditions. The Fig.6 shows the design of SEPIC converter along with the Matlab function for implementation of the proposed MPPT algorithm.

The Incremental conductance based maximum power point tracking algorithm is built in the Matlab function generator block using the code. The code for the Incremental conductance based MPPT logic which is developed in the C language and built in the Matlab function. The flow chart is shown in the Fig.7.

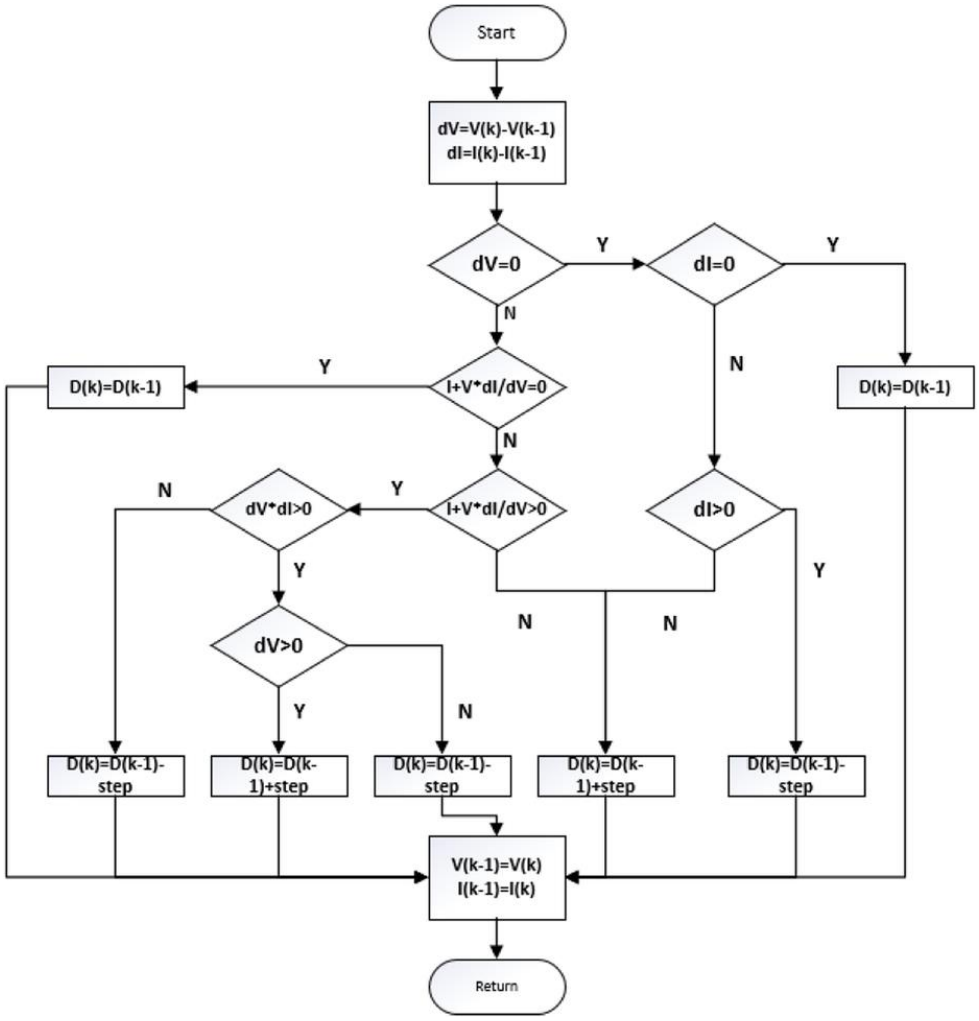

Fig.7 Incremental Conductance based MPPT algorithm built in Matlab function

B. Simulation of VSI and LCL filter

The inverter utilized for simulation is developed using the insulated-gate bipolar transistor (IGBT). The amount of DC converted to AC is determined by the conversion percentage. The IGBT is triggered using the pulse width modulation (PWM) method, which converts DC to AC. Fig.8 depicts the VSI developed in Matlab/Simulink that is employed as a 3-level IGBT in this project.

This work is licensed under a Creative Commons Attribution 4.0 International License

IJIREEICE
ISSN (Online) 2321-2004
ISSN (Print) 2321-5526
International Journal of Innovative Research in
Electrical, Electronics, Instrumentation and Control Engineering
Vol. 9, Issue 6, June 2021
DOI 10.17148/IJIREEICE.2021.9636

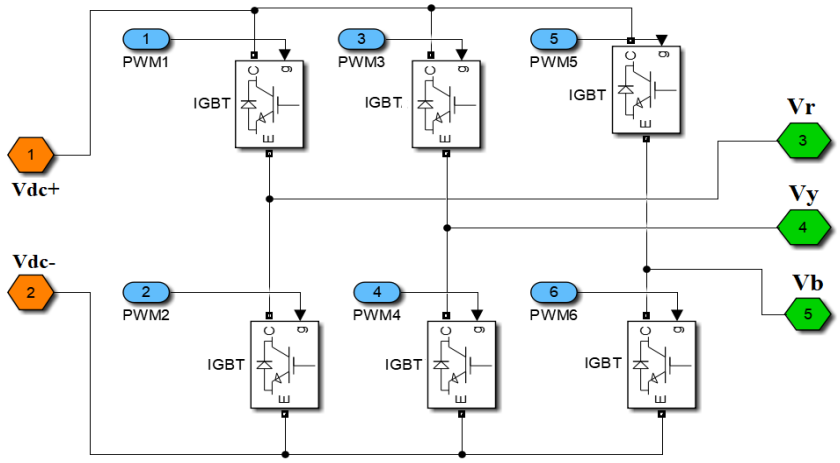

Fig.8 IGBT based Three phase Voltage Source Inverter

The Fig.9 depicts the inverter of the proposed model that is connected to the common DC connection (Vdc+ & Vdc-). The electric power supply is transferred into the grid by the interface mechanism of the DC bus and the three-stage AC grid, followed by the LCL filter.

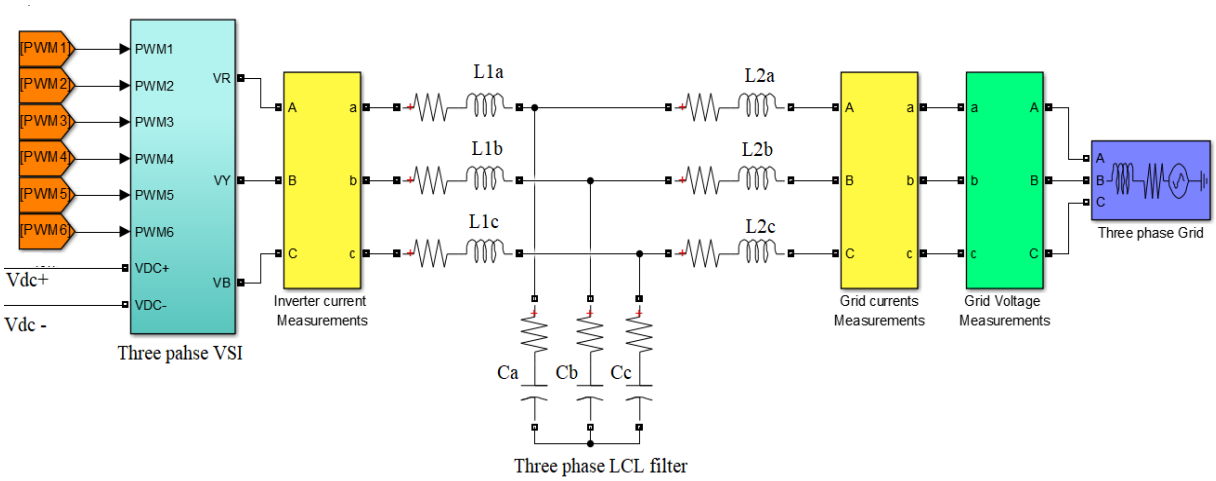

Fig.9 Simulation of the VSI, Filter and measurements blocks

C. Implementation of Controller for VSI

Both reactive and active power can be controlled separately via VSC converters. The active power reference is changed in a renewable energy network, such as a PV system, to manage the DC bus voltage and maintain power balance. As a result, the amount of energy put into the system will be equal to the amount of power generated.

The converter's control system is depicted in Fig.10. A two-level cascaded control scheme underpins it. The reference current loop's inner level controller regulates the AC current, while the reference voltage loop's outer level controller regulates the DC bus voltage.

This work is licensed under a Creative Commons Attribution 4.0 International License

IJIREEICE
ISSN (Online) 2321-2004
ISSN (Print) 2321-5526
International Journal of Innovative Research in
Electrical, Electronics, Instrumentation and Control Engineering
Vol. 9, Issue 6, June 2021
DOI 10.17148/IJIREEICE.2021.9636

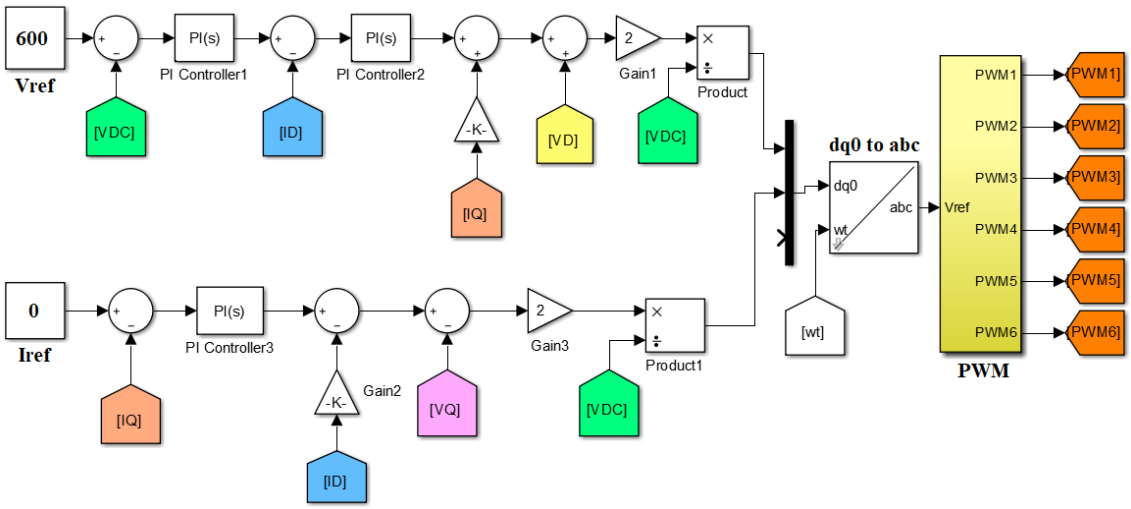

Fig.10 Current and Voltage controller for VSI

To vary the electrical grid angle, several controllers deal with current and voltages in the qd0 rotating two-axis reference frame. As a result, the grid angle must be monitored using a phase locked loop (PLL).
The inverter's IGBT switches on and off time is monitored by gate control signals. These signals are generated by the inverter control loop. The inverter control configuration consists of the following steps,

1. **Phase looked loop:** A phase-locked loop (PLL) is used to determine the frequency and phase of the grid that is connected proposed system.
2. **DC voltage control loop**: This voltage loop is used for DC bus voltage control and to ensure the power balance between PV and grid-injected power.
3. **Current Control loop:** This is programmed to analyze the voltages to be used by the VSC in order to guarantee that the currents flowing through the converter match the controller's voltages.
4. **Voltage Modulation:** The anti-park transformation block converts voltages computed from the current loop in the dq0 reference frame into the abc reference frame, which is then immediately inserted into the regulated voltage sources modeled on the AC converter side.

The voltage control unit and the current control unit make up the control system. The control system output signal is fed into the PWM signal generator, which uses the pulse to drive the grid end converter. $V_{dc(ref)}$ is compared to each sample, and the grid voltage is calibrated for the correct voltage for each sampling period V_{dc}. Where V_{dc} is DC-link tension, $V_{dc(ref)}$, is DC-link tension of reference, and $V_{dc(error)}$ is DC-link tension error.

The d and q axis components are referenced by I_{dref} and I_{qref} , respectively and the K_{p_vdc}, K_{i_vdc} are the proportional and integrated PI controller constants. The current regulators PI controller K_{p_cr}, K_{i_cr} are 0.3 and 20 for V_d and V_q respectively. For the three-phase grid current I_{abc_grid}, the d and q current components are the I_d and the I_q, respectively. The control voltage $V_{control\_grid}$ used for PWM generation is obtained by applying a transformation to provide V_d and V_q.

The inverter's controller, as illustrated in Figure 5.6, is grid-connected, meaning it operates at the grid's voltage and frequency. ABC coordination is used on the inverter side to measure current and voltage and pass through a step-by-step lock loop. This abc frame to d-q frame transformation is known as an asynchronous framework, and three-phased parameters are transformed into two-phase parameters. The phase angle is denoted by the PLL. In the simulation, a three-stage VSC converts 600 V DC to 400 V AC. To reduce the harmonics generated by this VSC, a 100 KVAR condenser bank filter is used.

This work is licensed under a Creative Commons Attribution 4.0 International License

IJIREEICE
ISSN (Online) 2321-2004
ISSN (Print) 2321-5526
International Journal of Innovative Research in
Electrical, Electronics, Instrumentation and Control Engineering
Vol. 9, Issue 6, June 2021
DOI 10.17148/IJIREEICE.2021.9636

D. The Phase-Locked Loop (PLL) and the dq0 Transformer

The signals are converted to the dq0 frame, which allows for precise control. Voltage and currents are converted to per-circuit values in this inverter control section. The grid voltage is sensed by PLL that determines its frequency and angle. It is critical for balancing the output and grid angles of the inverters. The dq0 transformer converts three-phase voltages and currents from abc to the reference frame.

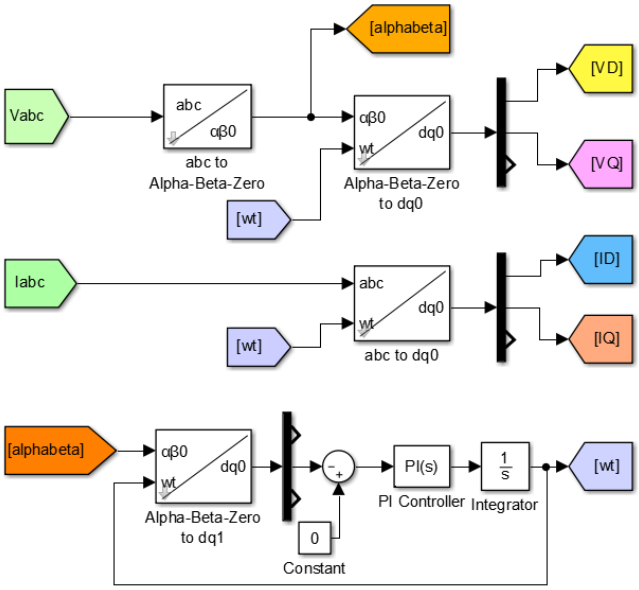

Fig.11 Phase-Locked Loop (PLL) and the dq0 & αβ0 Transformer

Fig 5.7 shows the PLL, which is utilized to synchronize the inverter with the Grid Line. The phase angle difference between the inverter voltage (V_{inv}) and the grid voltage (V_{grid}) is reduced to zero with the PLL control. Accurate synchronization control can be accomplished to display noise relative to the grid by detecting grid voltage in a phase-locked loop. The current angle of the grid voltage is the PLL output. Through managing δ, the actual and reactive power flux to the gridline can be obtained:

$$P = \frac{V_{inv} \cdot V_{grid}}{X_L} sin\,\delta \tag{12}$$

$$Q = \frac{V_{inv}}{X_L}(V_{inv} - V_{grid}\,cos\,\delta) \tag{13}$$

The reactive and active power of the system is shown in Equation (12) & (13). The impedance associated with the transformer leaking is denoted by X_L. The hybrid operating system's major concerns are device reliability and control efficiency. By enhancing the inverter pulse control and synchronization procedure, these concerns for the grid connected option can be greatly reduced.

E. Pulse Width Modulation (PWM)

The referenced voltages can be used by the VSC converter by modulating them with pulse width modulation (PWM). IGBT switching cycle is determined by modulation. One of the easiest approaches for incorporating PWM is sinusoidal pulse width modulation (SPWM) and it is depicted in the Fig.12.

This work is licensed under a Creative Commons Attribution 4.0 International License

IJIREEICE
ISSN (Online) 2321-2004
ISSN (Print) 2321-5526
International Journal of Innovative Research in
Electrical, Electronics, Instrumentation and Control Engineering
Vol. 9, Issue 6, June 2021
DOI 10.17148/IJIREEICE.2021.9636

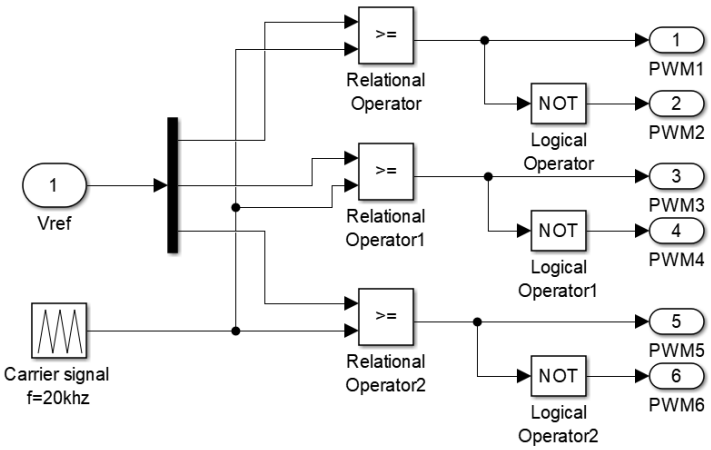

Fig.12 Sinusoidal pulse width modulation block

SPWM distinguishes between the two signals i.e., desired signal or a modulating signal, and a triangular signal considered as a carrier signal. The comparison of the two signals results in a square waveform signal containing a replica of the desired signal. The IGBT switching frequency will be the carrier signal frequency. This technique enables easy signal filtering with good results. Higher carrier frequency allows more accurate switching, but often implies a greater number of changes per cycle and thus increased power loss.

In designing the SPWM, two parameters must be considered: the modulation index and the carrier, as given in Equation (14). Further the relationship between the modulation signals frequency and the carrier is as indicated in Equation (15).

$$m = \frac{A_m}{A_c} \leq 1 \tag{14}$$

$$n = \frac{f_m}{f_c} = 3k \ (k \in N) \tag{15}$$

By controlling the modulation index, the amplitude of the applied output voltage can be regulated. If the modulation index is greater than one, it implies the over modulation. Usually, the switching frequency within the range of 215 kHz is considered that is sufficient for power system applications.

V. SIMULATION OF PROPOSED SYSTEM

MATLAB/Simulink software is used to model and simulate the proposed two-stage three phase grid connected inverter. Both the quality of the current injected into the grid and the MPPT performance of the proposed system are investigated. As a result, different operating circumstances such as constant irradiation, variable irradiation, and a step change in irradiation level have been considered.

The system and control parameters used in the simulation study are given in Table 4.

TABLE IV System and Control Parameters

Sl no	Parameters	Symbols	Values & units
1	Module type	47parallel x 10series	1Soltech 1STH-215-P
2	MPP of the PV array	*kW*	100 kW
3	Open Circuit Voltage of PV	V_{oc}	290 V
4	MPP Voltage of PV	V_{mpp}	363 V
5	SEPIC-side inductance	*La & Lb*	28.3 µH
6	SEPIC-side capacitance	*C1 & C2*	4000 µF
7	Step size constant value	*k*	0.00002

This work is licensed under a Creative Commons Attribution 4.0 International License

IJIREEICE
ISSN (Online) 2321-2004
ISSN (Print) 2321-5526
International Journal of Innovative Research in
Electrical, Electronics, Instrumentation and Control Engineering
Vol. 9, Issue 6, June 2021
DOI 10.17148/IJIREEICE.2021.9636

8	DC link reference voltage	V_{in}	600 V
9	Filter Inductance	L_1 *and* L_2	500 µH
10	Filter capacitance	*Ca, Cb, Cc*	100 µF
11	Grid voltage amplitude	*Vg*	230√2 V
12	Grid frequency	*fg*	50 Hz
13	Switching frequency of PWM	*fsw*	20 kHz
14	Current reference generation	*Kp & Ki*	10 & 1
15	Voltage reference generation	*Kp &Ki*	0.005 & 0.007

Fig.13 depicts a comprehensive PV-grid system simulation with a total power of 100 KW and 470 solar modules under STC. The PV array contains 47 parallel strings and 10 series strings in the system.

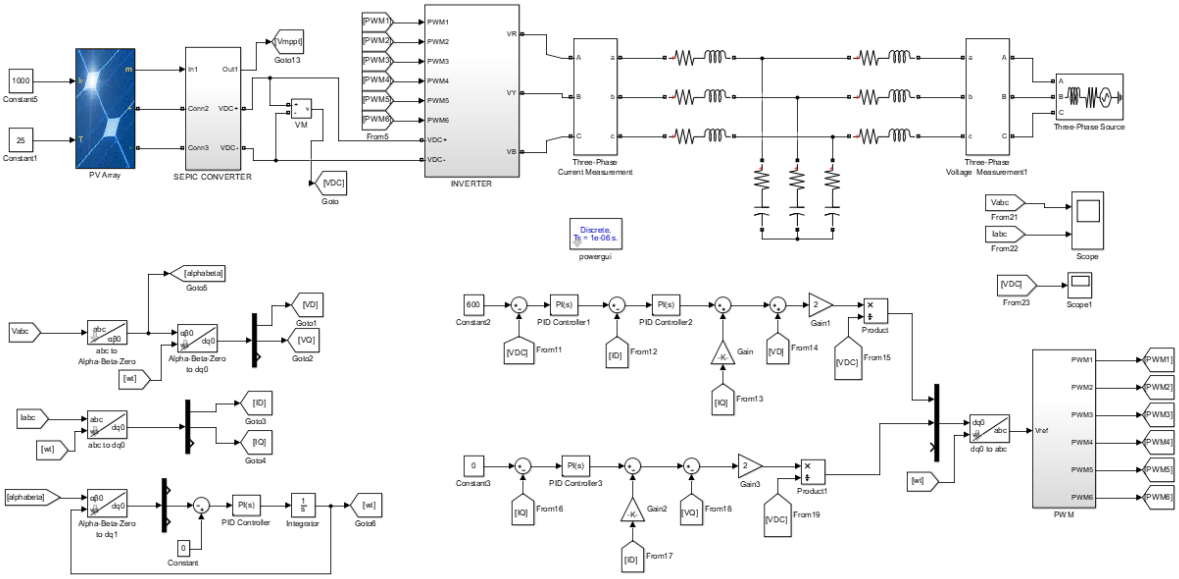

Fig.13 Simulation circuit of Proposed System.

A. Simulation results for constant Irradiation level and Temperature

The simulation is carried out for the constant Irradiation level of 1000W/m^2, at standard temperature condition (STC) of 25°C. The Fig.14(a) shows the Maximum power of the PV module for the Irradiation of 1000W/m^2. The power obtained at the grid side for the applied irradiation is shown in the Fig.14(b).

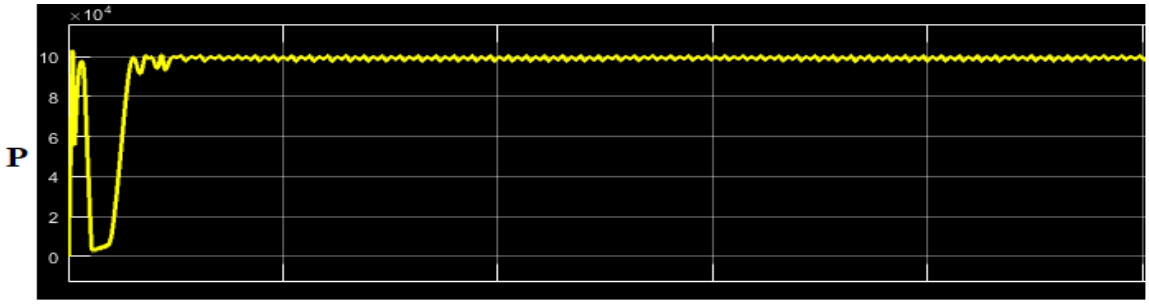

(a)

This work is licensed under a Creative Commons Attribution 4.0 International License

IJIREEICE

ISSN (Online) 2321-2004
ISSN (Print) 2321-5526

International Journal of Innovative Research in
Electrical, Electronics, Instrumentation and Control Engineering

Vol. 9, Issue 6, June 2021

DOI 10.17148/IJIREEICE.2021.9636

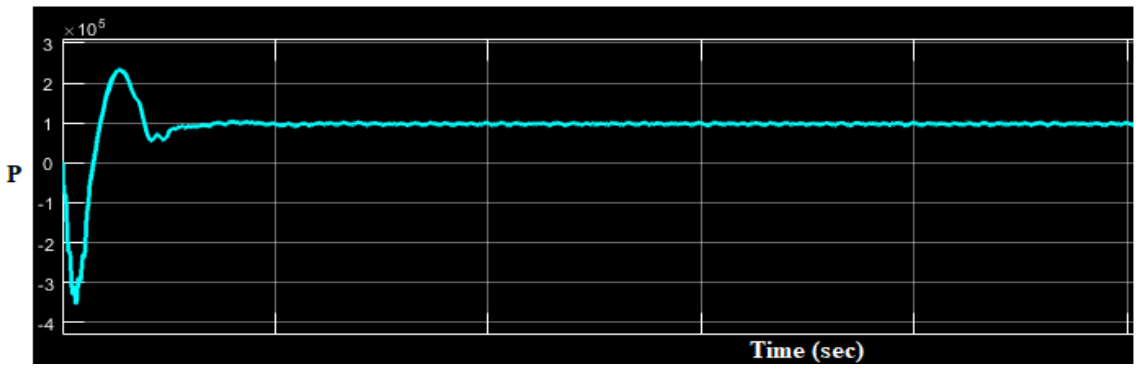

(b)

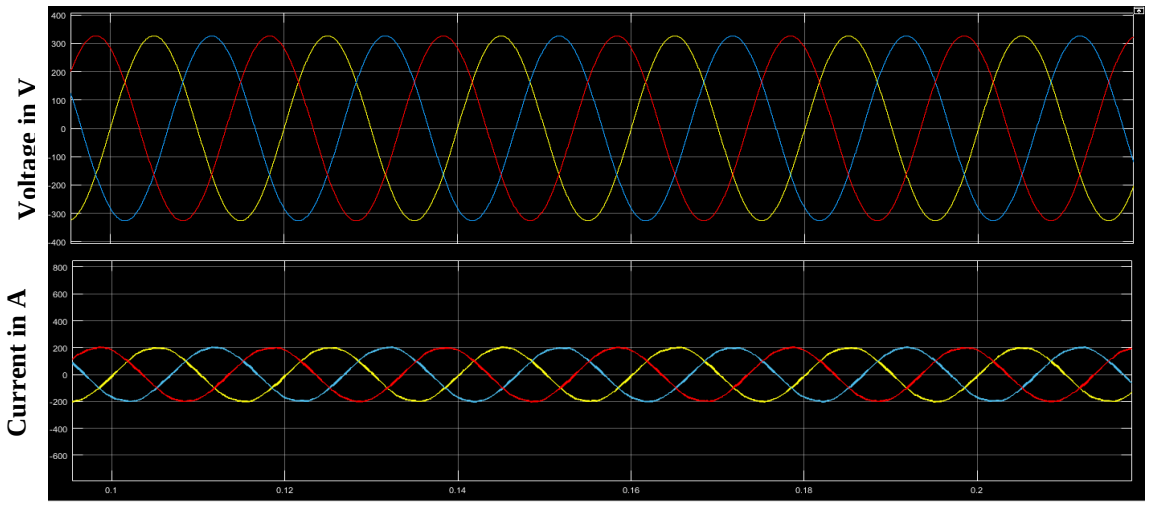

(c)

Time in sec

Fig.14 (a) MPP of the PV array, (b) Power output of complete system, (c) 3ph Grid Voltage, (d) 3ph Grid Current for constant Irradiation of 1000W/m^2 at STC of 25°C.

The grid voltage and current for the applied irradiation and temperature is show in the Fig.14(c & d) respectively, the waveform in the Fig.14(c & d) also depicts that the voltage and current obtained at the grid side is more active in nature that helps to pump the active power into the grid and in turn increases the power factor and overall efficiency of the complete system.

B. Simulation results for varying Irradiation level & constant Temperature

The dynamic performance of the proposed MPPT scheme and grid connected PV system is tested for varying Irradiation level and constant temperature. The Fig.15(a) depicts the variation of radiation level, Fig 6.3(b) depicts the MPP of the PV array and Fig 6.3(c) shows the amount of output power extracted from the PV system.

This work is licensed under a Creative Commons Attribution 4.0 International License

IJIREEICE

ISSN (Online) 2321-2004
ISSN (Print) 2321-5526

International Journal of Innovative Research in
Electrical, Electronics, Instrumentation and Control Engineering

Vol. 9, Issue 6, June 2021

DOI 10.17148/IJIREEICE.2021.9636

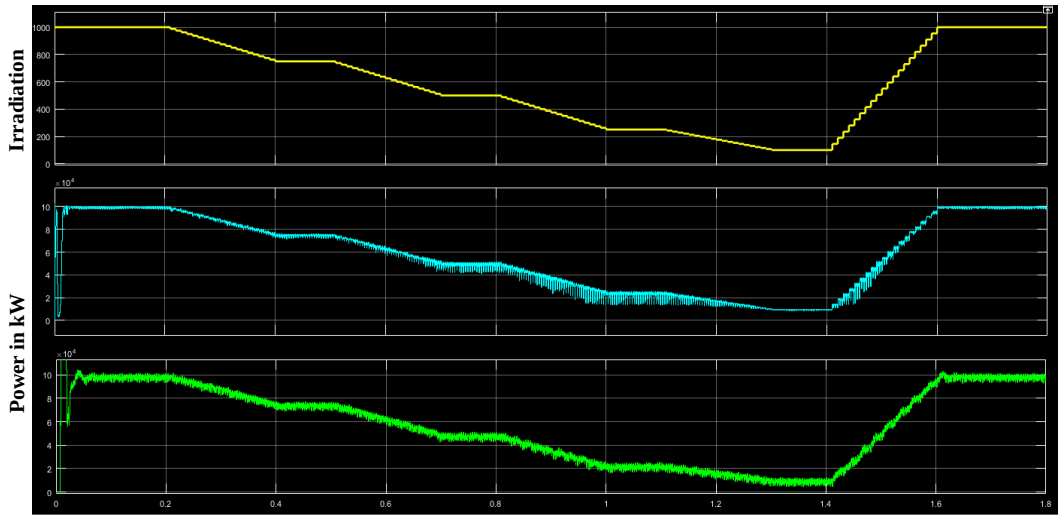

Fig.15 (a) Variation of radiation level, (b) MPP of the PV array, (c) Total output power extracted from the PV system.

The simulation starts at t = 0 when irradiance is 1000W/m^2, and the temperature is 25 °C , at the irradiance of 1000W/m^2 that is considered as systems maximum irradiance, MPP of the PV array and the maximum output power of 100kW & 98.71kW respectively is extracted from PV array. From t = 0.2s, the solar irradiance reduces to 750W/m^2 hence the incident solar energy reduces, and the MPP of the PV array reduces to 74.86kW, also the output power reduces from 98.7 kW to 73.98kW.

Further at t = 0.7s the Irradiation level is ramped down to 500 W/m^2 causing the MPP of the PV panel and Output power of the system to reduce to the value of 49.5kW & 48.27kW respectively. Finally at t = 1.3s the solar irradiation is ramped down to 100W/m^2, resulting in further reduction of MPP of PV to 9.73kW and Maximum system output power to 9.71kW.

TABLE V, Values of different parameters for varying irradiation with STC

Sam -ple	Temperature in ºC	Radiation (W/m^2)	MPP Theoretical (kW)	MPP Measured (kW)	Output Power (kW)	DC Bus Voltage (Vdc)	Iabc (peak) (Amps)	Vabc (peak) (Volts)
1	25	1000	**100.02**	**99.51**	98.71	600	199	400
2	25	750	**70.58**	**74.86**	73.98	600	148	400
3	25	500	**50.07**	**49.49**	48.27	600	99	400
4	25	250	**20.51**	**24.67**	23.76	600	49	400
5	25	100	**9.72**	**9.73**	9.71	600	25	400
6	25	1000	**100.02**	**99.24**	98.14	600	199	400

Therefore, irradiance is directly proportional to power generated, hence reducing irradiance will reduce the performance of the system. The Table.5 shows the detail tabulation for the simulation results of the waveforms shown in the Fig.15. The values of the different parameters with the variation of solar Irradiation and constant temperature will affect the MPP of PV array and output power pumped into grid. The MPP for the PV module is tracked for the different

This work is licensed under a Creative Commons Attribution 4.0 International License

IJIREEICE
ISSN (Online) 2321-2004
ISSN (Print) 2321-5526
International Journal of Innovative Research in
Electrical, Electronics, Instrumentation and Control Engineering
Vol. 9, Issue 6, June 2021
DOI 10.17148/IJIREEICE.2021.9636

Irradiation level and the power pumped into grid follows the Maximum power of the PV, which verifies the successful implementation of the proposed INC MPPT technique and current control technique of the VSI respectively.

C. Simulation results for Varying Temperature & Constant Irradiation level

The dynamic performance of the proposed MPPT scheme and grid connected PV system is tested for change in internal temperature of the PV module and constant irradiation. The Fig.16(a) depicts the variation of internal PV module temperature, Fig.16(b) depicts the MPP of the PV array and Fig.16(c) shows the amount of output power extracted from the PV system.

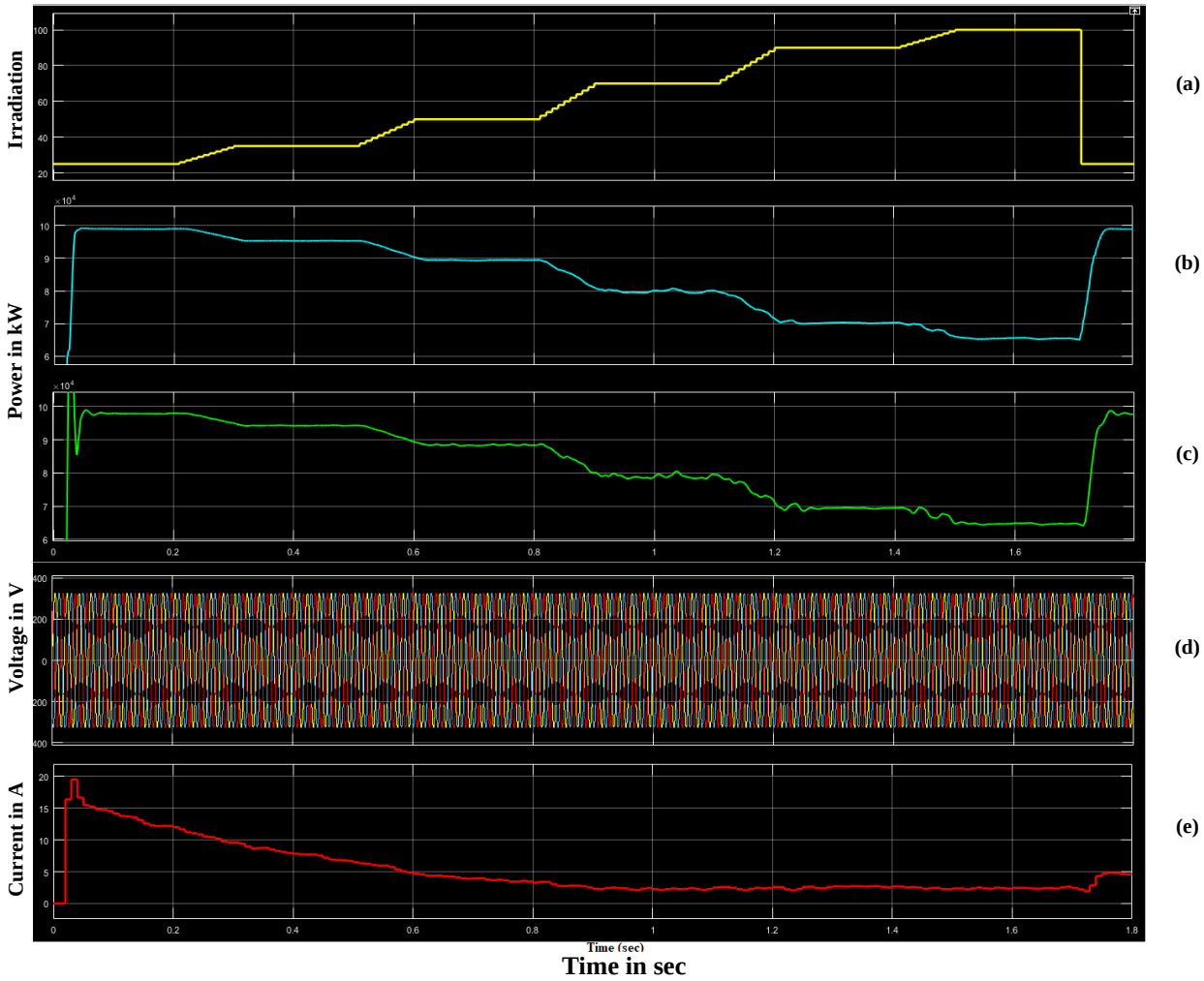

Fig.16 (a) Variation of PV cell internal temperature, (b) MPP of the PV array, (c) Total output power extracted from the PV system. (d) 3ph grid voltage, (e) Grid side current

The simulation starts at t = 0 when PV internal temperature is 25 °C and irradiance is 1000W/m^2, at the temperature of 25 °C which is the STC, MPP of the PV array and the maximum output power of 98.95kW & 97.881kW respectively is extracted from PV array. From t = 0.6s, the PV internal temperature is increased to 50°C, the MPP of the PV array reduces to 89.46kW, also the output power reduces from 97.88 kW to 88.38kW.

Further at t = 0.9s the internal temperature of the PV module is ramped upped to 70°C, causing the MPP of the PV panel and Output power of the system to reduce to the value of 80.07kW & 78.91kW respectively. Finally at t = 1.5s the PV internal temperature is ramped upped to maximum operating temperature of 100°C, resulting in further reduction of MPP of PV to 65.5kW and Maximum system output power to 64.84kW.

This work is licensed under a Creative Commons Attribution 4.0 International License

IJIREEICE
ISSN (Online) 2321-2004
ISSN (Print) 2321-5526
International Journal of Innovative Research in
Electrical, Electronics, Instrumentation and Control Engineering
Vol. 9, Issue 6, June 2021
DOI 10.17148/IJIREEICE.2021.9636

The Fig.16(d & e) shows the waveform of three phase grid side voltage and variation in injected current into the grid for the variation of the PV internal temperature.

TABLE VI, Values of different parameters for varying Temperature & fixed Irradiation

Samples	Radiation (W/m^2)	Temperature in ^oC	MPP Theoretical (kW)	MPP Measured (kW)	Output Power (kW)	Output Voltage of PV Array (Vin)	Output Current of PV Array (A)	DC Bus Voltage (Vdc)
1	1000	25 ^oC	**100.02**	**98.95**	97.88	290	342	600
2	1000	35 ^oC	**95.99**	**95.35**	94.23	276	344	600
3	1000	50 ^oC	**89.71**	**89.46**	88.38	286	348	600
4	1000	70 ^oC	**81.07**	**80.07**	78.91	230	338	600
5	1000	90 ^oC	**72.17**	**70.25**	69.42	204	322	600
6	1000	100 ^oC	**67.64**	**65.5**	64.84	191	318	600

Therefore the change in temperature also has a significant impact on the output voltage and output current from the PV array. The above simulation results and tabulation of the results in Table.6 clearly show the increase in temperature decreases the performance of the PV panels.

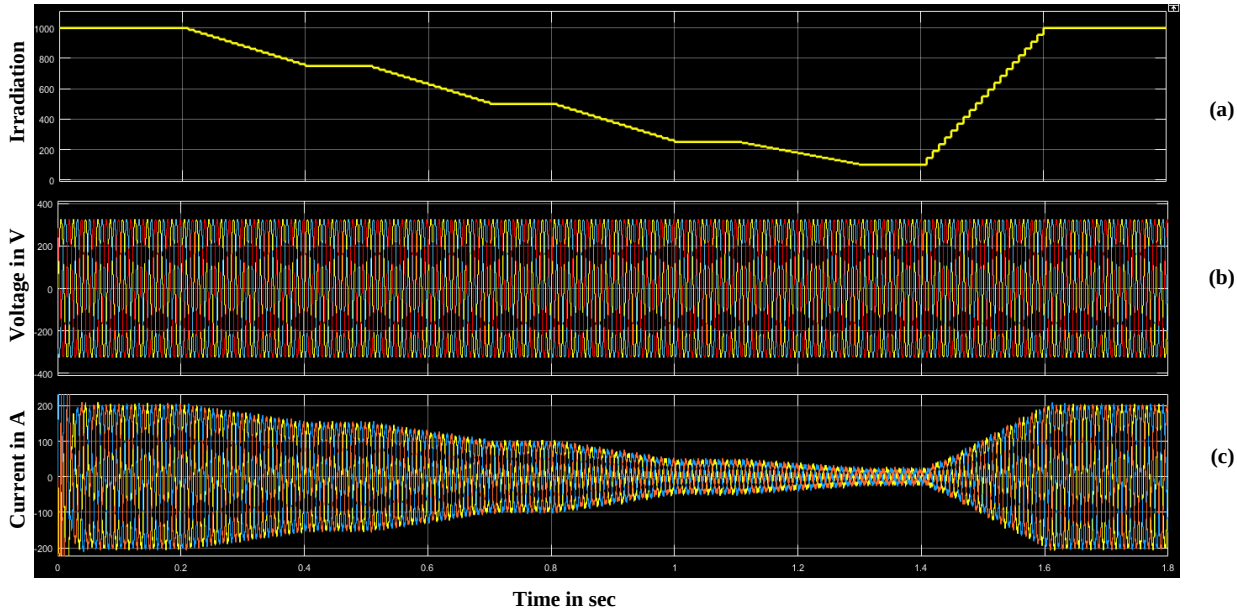

Fig.17 (a) Variation in irradiation, (b) Grid Voltage, (c) Grid current

The proposed SMC scheme's dynamic performance is also evaluated. At t=0.2s, 0.4s, 0.6s, 0.8s, 1s and 1.2s the reference amplitude value of the grid current is subjected to a step variation. Fig.17 depicts the inverter and grid side currents, as well as the grid voltage waveforms. It is clear that the proposed SMC-based current control technique has a very quick transient response and that the grid currents successfully track their reference currents.

This work is licensed under a Creative Commons Attribution 4.0 International License

IJIREEICE

ISSN (Online) 2321-2004
ISSN (Print) 2321-5526

International Journal of Innovative Research in
Electrical, Electronics, Instrumentation and Control Engineering

Vol. 9, Issue 6, June 2021

DOI 10.17148/IJIREEICE.2021.9636

D. Effect of the output filter

It is seen from the current waveforms in the Fig .18, the grid currents are sinusoidal waveform and waveform distortion levels is very low in the output of the filtered current (Fig 18c) when compared to the output current waveform of the inverter (Fig.18b). The total harmonic distortion (THD) level of the grid currents is computed to be 1.41% as shown in the Fig.19 that meets the international standards such as IEEE1547, IEC 61727 and AS4777.

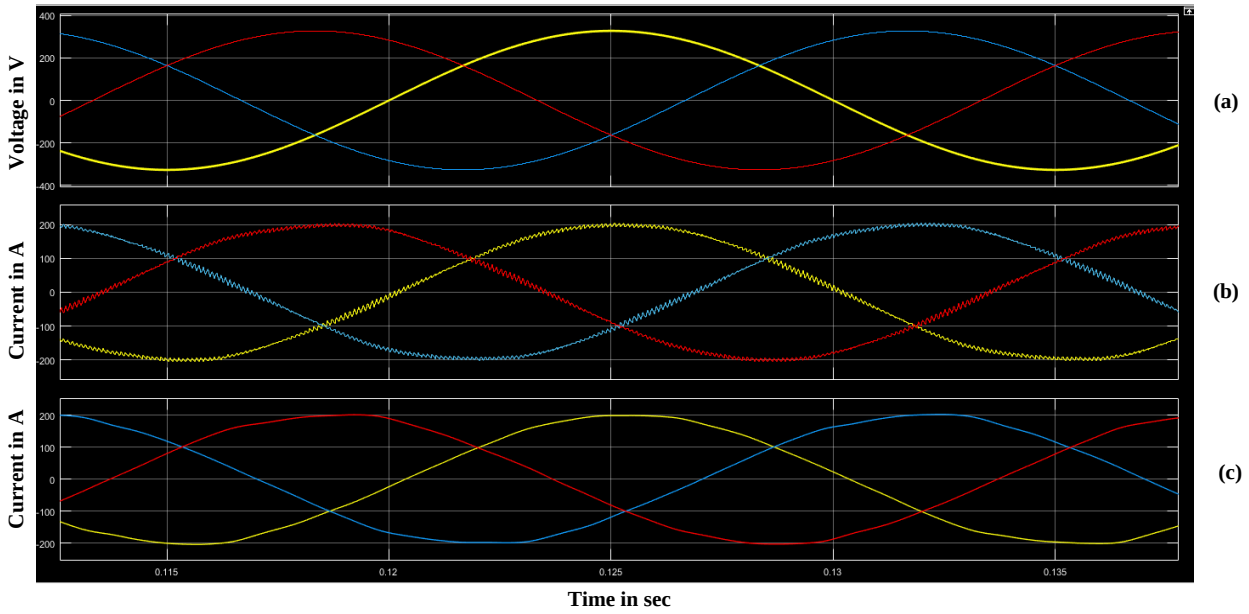

Fig.18 (a) 3ph grid voltages, (b) 3ph Inverter side currents, (c) 3ph Filter output currents

Furthermore from Fig.18(b) & (c), it is verified that both current waveforms show no oscillation, indicating that there is sufficient damping. Finally form Fig.18(a) & (c) it is visible that the grid currents and grid voltages are in phase, resulting in unity power factor operation.

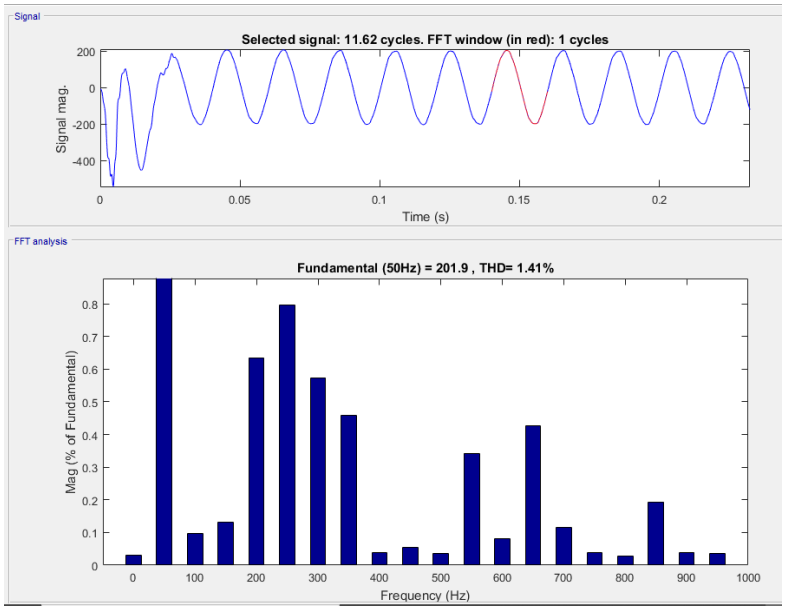

Fig.19 THD level of the grid current

E. Summary

MATLAB/Simulink is used to model and simulate the proposed two-stage inverter. Both the quality of the current injected into the grid and the MPPT performance of the proposed system are investigated. As a result, different

This work is licensed under a Creative Commons Attribution 4.0 International License

IJIREEICE

ISSN (Online) 2321-2004
ISSN (Print) 2321-5526

International Journal of Innovative Research in
Electrical, Electronics, Instrumentation and Control Engineering

Vol. 9, Issue 6, June 2021

DOI 10.17148/IJIREEICE.2021.9636

operating circumstances such as constant irradiation and temperature, variable irradiation and temperature, and a step change in irradiation level have been considered.

It is seen from the above simulation results, that the proposed two stage grid-connected inverter has fast start up and the MPP of the system is reached within short time. Besides, the proposed system has quick transient response at the step change instants. When the variation in irradiation and the output power of the PV system are compared, it is clear that they are in accord. It is concluded that the proposed MPPT algorithm and SMC-based current control scheme have the potential to track system operation points with high accuracy and without oscillations for any of the operation points.

VI. CONCLUSION

In order to improve the conventional system due to rapidly changing irradiation, this paper suggested an improved MPPT controller without measuring the produced PV array capacity. In simulation, the strong tracking capability of gradually rising and dropping irradiance is established. The proposed MPPT allows the power shift produced by the simultaneous rise in disturbance and variation in irradiation to be decoupled.

Dynamic tracking errors minimize output power losses considerably, especially under rapidly changing irradiation. An error in the PI DC voltage controller signal is used to determine the irradiation difference. At the constant ambient conditions, the PI regulator is designed to ensure zero signal error. As a result, the signal error is simply the difference in power caused by the irradiation variance. The total power shift in the PV array is previously measured using the d-axis grid current component. The overall shift in the PV array's power is then measured using the d-axis grid current component. The feasibility of a designed PV network capable of providing sufficient constant power to various AC loads under different environmental limitations, including irradiance and temperature, has therefore been investigated in this project.

A two-stage grid-connected inverter system for PV applications is proposed in this paper. A MPPT SEPIC converter, three-phase VSI, and a current control algorithm based on SMC build up the proposed system. The MPP of the system is tracked using the INC technique. Simulations in MATLAB/Simulink are used to evaluate the system's performance. The obtained results reveal that the grid currents injected into the grid are sinusoidal and have a very low level of distortion of less than 1.41%. The MPPT algorithm implemented in this project is fully capable in tracking the Maximum power point of the PV array for all the environmental conditions simulated in the project with minimum loses, this makes the system highly efficient in tracking MPP and efficiency of the system lies between 98%-99%. Further, the suggested system has a very quick transient response and excellent accuracy in all operating situations.

REFERENCES

[1]. Li. Y, Chen. C and Xie. Q, “Research of an improved grid-connected PV generation inverter control system”. In Proceedings of the 2010 International Conference on Power System Technology, Hangzhou, China, 24–28, pp. 1–6, October 2010.

[2]. Carrasco J.M., Franquelo L.G, Bialasiewicz, J.T, Galvan. E, Portillo Guisado R.C, Prats M.A.M., Leon .J.I and Moreno-Alfonso.N, “Power-electronic systems for the grid integration of renewable energy sources”. IEEE Trans. Ind. Electron, 53, 1002–1016, December 2016

[3]. Alepuz. S, Busquets-Monge S., Bordonau J, Gago J, Gonzalez D and Balcells J, “Interfacing renewable energy sources to the utility grid using a three-level inverter”. IEEE Trans. Ind. Electron., 53, 1504–1511, March 2006.

[4]. Calais M, Agelidis V.G, and Dymond, M.S, “A cascaded inverter for transformer less single-phase grid connected photovoltaic systems”. Renew. Energy, 22, 255–262, March 2001 .

[5]. Jamil M, Waris A, Gilani, S.O, Khawaja B.A, Khan M.N and Raza, “A. design of robust higher-order repetitive controller using phase lead compensator”. IEEE Access, 30603–30614, 2020.

[6]. Jamil M, Hussain B, Sharkh S.M and Abusara M.A, “Microgrid Power Electronic Converters: State of The Art and Future Challenges”. In Proceedings of the 44th International Universities Power Engineering Conference (UPEC), Glasgow, UK, 1–4, September 2009.

[7]. Altas I.H, and Sharaf A.M, “A photovoltaic array simulation model for matlab-simulink GUI environment”. In Proceedings of the 2007 International Conference on Clean Electrical Power, Capri, Italy, 21–23, pp. 341–345, May 2007.

[8]. Afroze S, Udaykumar R.Y and Naik A, “A systematic approach to grid connected PV system”. In Proceedings of the 2012 IEEE Fifth Power India Conference, Murthal, India, 19–22, pp. 1–5, December 2012.

[9]. Agelidis V.G, Baker D.M., Lawrance W.B. and Nayar C.V, “A multilevel PWM inverter topology for photovoltaic applications”. In Proceedings of the ISIE ’97 Proceeding of the IEEE International Symposium on Industrial Electronics, Guimaraes, Portugal, 7–11, Volume 2, pp. 589–594, July 1997.

[10]. Tung Y.M., Hu A.P. and Nair N.K. “Evaluation of micro controller based maximum power point tracking methods using dSPACE platform”. In Proceedings of the Australian University Power Engineering Conference, presented at Australasian Universities Power Engineering Conference (AUPEC 2006), Melbourne, Australia, 10–13 December 2006.

This work is licensed under a Creative Commons Attribution 4.0 International License

IJIREEICE

ISSN (Online) 2321-2004
ISSN (Print) 2321-5526

International Journal of Innovative Research in
Electrical, Electronics, Instrumentation and Control Engineering

Vol. 9, Issue 6, June 2021

DOI 10.17148/IJIREEICE.2021.9636

[11]. Challa D.T.R. and Raghavendar I. "Implementation of incremental conductance MPPT with direct control method using cuk converter". Int. J. Mod. Eng. Res. 2012, 2, 4491–4496, December 2012.

[12]. Suwannatrai P., Liutanakul P. and Wipasuramonton P., "Maximum power point tracking by incremental conductance method for photovoltaic systems with phase shifted full-bridge dc-dc converter". In Proceedings of the 8th Electrical Engineering/Electronics, Computer, Telecommunications and Information Technology (ECTI) Association of Thailand—Conference 2011, Khon Kaen, Thailand, 17–19, pp. 637–640, May 2011.

[13]. Xuesong Z., Daichun S., Youjie M. and Deshu C., "The simulation and design for MPPT of PV system Based on Incremental Conductance Method". In Proceedings of the 2010 WASE International Conference on Information Engineering, Beidaihe, China, 14–15, Volume 2, pp. 314–317, August 2010.

[14]. Satpathy. P.R., Jena S. and Sharma R., "Performance analysis of the perturb-and-observe and incremental conductance MPPT under varying weather conditions". In Proceedings of the 1st International Conference on Large-Scale Grid Integration of Renewable Energy, New Delhi, India, 6–8 September 2017.

[15]. Jaalam N., Rahim N.A., Bakar A.H.A., Tan C.K. and Haidar M.K., "A comprehensive review of synchronization methods for grid-connected converters of renewable energy source". Renew. Sustain. Energy Rev. 2016, 59, 1471–1481.

[16]. Jamil M., Arshad R., Rashid U., Gilani S.O., Ayaz Y. and Khan M.N., "Robust repetitive current control of two-level utility connected converter using LCL filter". Arab. J. Sci. Eng., 40, 2653–2670. June 2015.

[17]. Prakash S. and Mishra S., "VSC control of grid connected PV for maintaining power supply during open-phase condition in distribution network". IEEE Trans. Ind. Appl., 55, 6211–6222, October 2019.

[18]. De Brito M.A., Sampaio L.P. and Luigi G., "Comparative analysis of MPPT techniques for PV applications". In Proceedings of the 2011 International Conference on Clean Electrical Power (ICCEP), Ischia, Italy, 14–16, pp. 99–104, June 2011.

[19]. Lourenço L.F., Monaro R.M., Salles M.B., Cardoso J.R. and Quéval L., "Evaluation of the reactive power support capability and associated technical costs of photovoltaic farms' operation". Energies, 11, 1567, 2018.

[20]. Kumar S. and Singh B., "A multipurpose PV system integrated to a three-phase distribution system using an LWDF-based approach". IEEE Trans. Power Electron., 33, 739–748, 2018.

[21]. Mohan D.M., Singh B., and Panigrahi B.K., "A two-level 24-pulse voltage source converter based HVDC system for active and reactive power control". In Proceedings of the IEEE International Conference on Power Control Embedded System (ICPCES), Allahabad, India, pp. 1–5, 29 November–1 December 2010.

[22]. Mohan D.M., Singh B. and Panigrahi B.K., "Harmonic optimized 24- pulse voltage source converter for high voltage DC systems". IET Power Electron, 2, 563–573. 24, 2009.

[23]. Ma L., Ran W. and Zheng T.Q., "Modeling and control of three phase grid-connected photovoltaic inverter". In Proceedings of the 8th IEEE International Conference on Control and Automation (ICCA), Xiamen, China, 9–11, pp. 2240–2245, June 2010.

[24]. S. Bhattacharjee and B. J. Saharia, "A comparative study on converter topologies for maximum power point tracking application in photovoltaic generation," Journal of Renewable and Sustainable Energy, vol. 6, no. 5, p. 053140, Sep. 2014.

This work is licensed under a Creative Commons Attribution 4.0 International License